Two Classes of Actin Microfilaments Are Associated with the Inner Cytoskeleton of Axons

Karl R. Fath and Raymond J. Lasek

Bio-architectonics Center Medical School, Case Western Reserve University, Cleveland, Ohio 44106; and Marine Biological Laboratory, Woods Hole, Massachusetts 02543

Abstract. The distribution and length of actin microfilaments (MF) was determined in axoplasm extruded from the giant axons of the squid (*Loligo pealeii*). Extruded axoplasm that was separated from the axonal cortex contains ~92% of the total axonal actin, and 60% of this actin is polymerized (Morris, J., and R. Lasek. 1984. *J. Cell Biol.* 98:2064–2076). Localization of MF with rhodamine-phalloidin indicated that the MF were organized in fine columns oriented longitudinally within the axoplasm. In the electron microscope, MF were surrounded by a dense matrix and they were associated with the microtubule domains of the axoplasm. The surrounding matrix tended to obscure the MF which may explain why MF have rarely been recognized before in the inner regions of the axon. The axoplasmic MF are relatively short (number average length of 0.55 μm). Length measurements of MF prepared either in the presence or absence of the actin-filament stabilizing drug phalloidin indicate that axoplasm contains two populations of MF: stable MF (number average length of 0.79 μm) and metastable MF (number average length of 0.41 μm). Although individual axonal MF are much shorter than axonal microtubules, the combined length of the total MF is twice that of the total microtubules. Apparently, these numerous short MF have an important structural role in the architecture of the inner axonal cytoskeleton.

ACTIN microfilaments (MF)[1] are essential components in acto-myosin-mediated motility and in the architecture of many kinds of cells. In axons, ultrastructural studies have suggested that MF are abundant in the cortical region subjacent to the axonal plasma membrane and that they are few in number in the central regions that constitute most of the axonal volume (Metuzals and Tasaki, 1978; Hirokawa, 1982; Hodge and Adelman, 1983; Letourneau, 1983; Tsukita et al., 1986). Furthermore, fluorescent probes for actin stain the axonal cortex much more intensely than the central axonal regions (Spooner and Holladay, 1981; Letourneau, 1983; Shaw et al., 1981; Hirokawa, 1982). These observations have led to the widely accepted view that axonal MF are primarily cortical and that few, if any, are located in the central regions of the axon (for review see Pachter et al., 1984).

This idea that MF are negligible components of the central axonal cytoskeleton is not consistent with the results of physiological studies. For example, if MF in the central axon are disrupted, fast vesicle transport is impaired (Brady et al., 1984). Furthermore, autoradiographic analyses of radiolabeled slowly transported cytoskeletal elements indicate that MF and other components of slow component b are principally located in the central (noncortical) regions of axons (Heriot et al., 1985). These studies indicate that actin MF have an important role in the dynamic architecture of the central axon.

Quantitative biochemical analyses also indicate that MF are abundant in the central axonal cytoskeleton (Morris and Lasek, 1984). These studies show that axoplasm extruded from the squid giant axon contains a large amount of polymerized actin (Morris and Lasek, 1984). Specifically, actin constitutes 6% of the total protein in extruded axoplasm, and 60% of this actin appears to be polymerized in MF (Morris and Lasek, 1984). Based on these analyses of the amounts of cytoskeletal polymers in axoplasm, we estimate that in axoplasm the total length of all MF approaches the total length of all neurofilaments and that it exceeds the total length of all microtubules (Table I).

To better understand the architectural role of MF in axons, we analyzed the spatial organization of MF in extruded axoplasm. Our results support the proposal of Morris and Lasek (1984) that MF are abundant in the central cytoskeleton of the squid giant axon, and the observations provide new information about the detailed organization of the axonal cytoskeleton.

Materials and Methods

Isolation of Axoplasm and Biochemical Analysis

From 400–500-μm-diam squid giant axons, the axoplasm (axon cytoplasm)

1. *Abbreviations used in this paper*: MF, microfilaments; S-1, myosin subfragment.

Table I. Predicted Cytoskeletal Polymer Lengths in Axoplasm

Polymer	Total length	No./μm^2	No./μl
	$\mu m/\mu l$		
Actin filaments	3.2×10^{10}*	28	5.9×10^{10}
Microtubules	1.6×10^{10}‡	16	1.6×10^{8}
Neurofilaments	3.4×10^{10}§	34	3.4×10^{8}

Values were calculated using protein concentrations supplied by Morris and Lasek (1984). The number of filaments per μm^2 were calculated assuming that all filaments are axially oriented (number increases as deviation increases) and that the number of filaments in a cross section are approximately constant.
* Actin filament lengths were calculated assuming 0.36 monomers/nm (Korn, 1982) and an average filament length of 0.55 μm (see text).
‡ Microtubule lengths were calculated assuming 13 dimers/8 nm (Amos et al., 1976) using an average filament length of 100 μm (Bray and Bunge, 1981).
§ Neurofilament lengths were calculated assuming 30 subunits/50 nm and an average subunit mass of 97,500 using an average filament length of 100 μm (data not available, estimate could be in error by a factor of two or more).

was physically extruded from its plasma membrane and glial sheath as previously described (Morris and Lasek, 1982). Extrusion did not appear to disrupt cytoskeletal elements of the axoplasm, instead they were highly organized even at the edge of the axoplasm where it was sheared away from the axonal cortex (see Fig. 1; Hodge and Adelman, 1983). The maintenance of cytoskeletal organization suggested that there was no significant exchange of materials between the cortical and central axoplasm during extrusion. Apparently, the extruded axoplasm separated from the cortical axoplasm at a sharp boundary. A thin (0.5–1.0 μm) cortical rim of axoplasm remained attached to the sheath. Because the axons we used were 400–500 μm in diameter, the central, extruded axoplasm from these axons contains approximately 98–99% of the total axoplasm.

Extruded axoplasm was triturated with a teflon/glass homogenizer (Type O; Thomas Scientific, Philadelphia, PA) in 250 μl 0.5 M potassium iodide (KI), 10 mM Tris-HCl, pH 7.6 (KI buffer). The KI buffer was used to separate actin from collagen in the sheath because collagen interfered with the analysis of the sheath proteins in SDS-PAGE. The homogenate was incubated overnight at 4°C and centrifuged at 30,900 *g* for 1 h at 4°C. The supernatants were removed and the pellets washed with KI buffer and recentrifuged. The supernatants were combined and the proteins precipitated with 10% cold TCA. The precipitates and KI pellets were solubilized in sample buffer and analyzed by SDS-PAGE. The gels were stained with Coomassie Brilliant Blue and the proteins of interest were scanned densitometrically (for details of gel preparation and analysis see Morris and Lasek, 1984). Two-dimensional PAGE of axoplasm showed that actin is the only protein with a molecular mass of 43,000 D (data not shown; Morris and Lasek, 1984); thus, one-dimensional SDS-PAGE was suitable for quantitative analysis of actin.

Negative Staining and S-1 Decoration of Dispersed Axoplasm

Extruded axoplasm was gently dispersed in a teflon/glass homogenizer containing 200–500 μl of a physiological buffer (buffer X) at 18–20°C (Brady et al., 1984). The dispersed axoplasm was placed on an electron microscope grid and reacted with myosin subfragment 1 (S-1) at 0.4 mg/ml in standard salts solution (50 mM KCl, 5 mM $MgCl_2$, 6 mM $NaPO_4$ buffer, pH 7.2). The S-1 was the alpha-chymotryptic fragment (Weeds and Taylor, 1975) of rabbit skeletal muscle myosin (Scordilis and Adelstein, 1978) and contained no contaminating actin MF as assayed by SDS-PAGE and negative staining. The "decorated" MF were fixed with 1% glutaraldehyde in the standard salts solution and negatively stained with 2% aqueous uranyl acetate pH ~4.0. Several control grids in each experiment were either not reacted with S-1 or were rinsed before fixation with standard salts solution containing either 1 mM ATP or Na pyrophosphate. Micrographs were taken on either a Zeiss EM 10C or a JEOL 100CX electron microscope calibrated with a carbon replica.

Isolation of Axoplasmic Actin MF

Axoplasm (3–4 μl) was extruded into 500 μl buffer X containing 10 μM phalloidin (Boehringer Manneheim Biochemicals, Indianapolis, IN). Phalloidin prevents MF depolymerization and protects them against the inevitable shear stresses encountered in specimen handling (Dancker et al., 1975; Atkinson et al., 1982). The axoplasm was gently agitated for 4–5 h at 18–20°C then KI was added to a final concentration of 0.6 M. The chaotropic KI depolymerized the axonal microtubules and neurofilaments but the phalloidin-protected MF remained intact.

To selectively study the stable MF that are not sensitive to dilution of the monomer pool, axoplasm (3–4 μl) was extruded into 500 μl buffer X lacking phalloidin. The axoplasm was extracted 4–5 h at 18–20°C, then transferred to a new solution of buffer X containing 10 μM phalloidin, incubated 30 min, and dispersed with 0.6 M KI.

Measurement of Axoplasmic MF Lengths

To measure the lengths of negatively stained MF, electron micrographs were taken of nonselected regions of the grid. Measurements of MF contour lengths were made from negatives at 16,000 or 20,000 magnifications with a calibrated ocular in a Wild dissecting microscope. It was possible to accurately identify and measure MF as short as 40–50 nm. Filament lengths were expressed as either filament number average or filament weight average (Cooper and Pollard, 1982). This method has proven useful for measuring MF polymerized in vitro (Kawamura and Maruyama, 1970) and for MF isolated from cells (Atkinson et al., 1982; Shen et al., 1984).

To determine if there was any artifactual lengthening of MF during specimen preparation axoplasm was extracted for several hours in buffer X minus Mg^{++} and Ca^{++} and containing 15 mM EDTA and 10 mM EGTA. In these conditions, actin monomer rapidly becomes nonpolymerizable (Korn, 1982). Then phalloidin was added and the axoplasm was dispersed with KI and negatively stained as above. Previous analyses of the amount of polymerized actin in axoplasm by the kinetic elution paradigm has shown that phalloidin does not increase the amount of polymerized actin in axoplasm (Morris and Lasek, 1984).

To assess the degree of filament fragmentation due to specimen handling, purified actin filaments were processed in parallel with axonal MF. Rabbit muscle actin was polymerized in buffer X containing 1 mM ATP. The filaments were processed in three different ways: (*a*) phalloidin (in 1% DMSO) was added to a final concentration of 10 μM; (*b*) 1% DMSO without phalloidin; and (*c*) no additions. The filaments from all three conditions were placed on a grid, fixed, and negatively stained.

Ultrastructure of Axoplasm

In some cases, axoplasm was directly extruded into fixative (see below). In other cases, axoplasm was extruded into buffer X containing 10 μM phalloidin and extracted with gentle stirring at 18–20°C for 4 h then transferred to fixative. Fixation was by immersion in 1% glutaraldehyde, 5 mM $MgCl_2$, 5 mM EGTA, 1 M sucrose, 0.1 M $NaPO_4$, pH 7.2–7.4 for 30 min. The following steps were chosen for the optimal preservation and visualization of MF as determined by McDonald (1984). The fixed axoplasm was washed for 5 min with $NaPO_4$ buffer (pH 7.2–7.4), reacted with 0.8% $K_3Fe(CN)_6$ in 0.1 M $NaPO_4$ for 5 min, then postfixed with 0.5% OsO_4, 0.8% $K_3Fe(CN)_6$ in $NaPO_4$ for 15 min on ice in the dark. It was then treated with 0.5% tannic acid (type 1764; Mallinckrodt, Inc., St. Louis, MO) in 0.1 M $NaPO_4$ for 5 min and rinsed in deionized water. The axoplasm was en bloc stained with 2% aqueous uranyl acetate, dehydrated through graded acetones, and embedded in Poly/Bed 812. Sections were stained with aqueous uranyl acetate and lead citrate.

S-1 Decoration of MF in Intact Axoplasm

Axoplasm was extruded into 500 μl buffer X containing 10 μM phalloidin at 18–20°C. The buffer was stirred gently for 2 min to allow endogenous ATP to elute from the axoplasm. The axoplasm was transferred to a new 250-μl buffer X/10-μM phalloidin solution containing 2 mg/ml S-1. The buffer was gently stirred for 6 min to allow S-1 penetration into the axoplasm, then the axoplasm was washed for 1–2 min in 500 μl of new buffer X/10 μM phalloidin to remove unbound S-1 and fixed as outlined above. In another protocol, axoplasm was extruded onto a dry coverslip and extracted 15 min with buffer X diluted 1:1 (vol/vol) with deionized water and containing 10 μM phalloidin. The solution was replaced with 1.5 mg/ml S-1 in diluted buffer X/10 μM phalloidin and incubated at 18–20°C for 20 min. The axoplasm was then washed with diluted buffer X/10 μM phalloidin for 15 min to remove unbound S-1 and fixed as above. Control experiments using both labeling protocols either omitted S-1 or contained 5 mM ATP in all solutions.

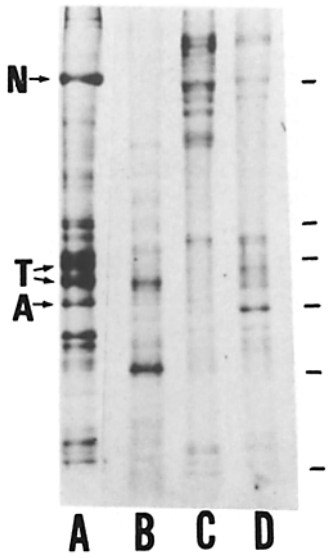

Figure 1. One dimensional SDS-PAGE of the proteins from one extruded axon. *Axoplasm A*, proteins from the KI supernatant; *B*, KI pellet from extruded axoplasm. *Sheath C*, proteins from the KI pellet; *D*, the KI supernatant from the sheath. The respective lanes were loaded for optimal separation, therefore a smaller fraction of the total axoplasmic proteins was loaded than were the sheath proteins. Several of the axonal proteins are actin (*A*), tubulin (*T*), and the neurofilament 200,000-D subunit (*N*). Actin was identified by M_r and specific recognition on Western blots with a monoclonal actin antibody, data not shown. The bars on the right indicate the mobilities of the molecular mass standards of 14,000, 30,000, 43,000, 57,000, 68,000, and 200,000 D, respectively.

Rhodamine-Phalloidin Staining of Axoplasm

Extruded axoplasm was fixed with 2% paraformaldehyde in buffered Ca^{++}-free artificial sea water (437 mM NaCl, 9 mM KCl, 22.94 mM $MgCl_2$, 25.5 mM $MgSO_4$, 100 mM $NaPO_4$ buffer, pH 7.4) for 20 min at 18–20°C. The axoplasm was washed twice for 15 min with PBSa (Dulbecco's Phosphate Buffered Saline without Ca^{++} or Mg^{++}; Gibco Laboratories, Grand Island, NY) and stained for 20 min with 0.1 μM rhodamine-phalloidin (Molecular Probes, Junction City, OR) in PBSa. After two 15-min PBSa washes the axoplasm was mounted in a glycerol and PBSa mixture (1:1) with the cover glass elevated from the slide by No. 1 cover glass fragments and sealed with VALAP (vaseline/lanolin/paraffin; 1:1:1). Photographs were taken on a Zeiss Photomicroscope III using epi-fluorescent illumination on Kodak Tri-X film at EI 1600 and developed with Accufine (Accufine, Inc., Chicago, IL).

Results

Quantitation of Actin in the Inner and Cortical Axoplasm

Fig. 1 indicates that extruded axoplasm contained a relatively high proportion of the total actin in the giant nerve fiber, and quantitative analyses of three axons demonstrated that 92% (SEM ± 3%) of the total axonal actin is located in the extruded axoplasm. Only 8% of the actin was located in the sheath, and a portion of this actin is in extra axonal cells. These results indicate that >92% of the actin in the squid giant axon is located within the inner axoplasm.

Identification of Actin MF and Length Measurements

To determine whether the actin in extruded axoplasm was assembled into MF, axoplasm was gently homogenized and negatively stained. Disrupted axoplasm contained many short 4–6-nm filaments that could bind S-1 in the arrowhead pattern characteristic of actin-containing MF (Fig. 2). These observations demonstrate that axoplasm contains actin MF and suggest that these MF are numerous.

Length is a fundamental parameter that can influence the function of MF. To measure MF length, phalloidin-stabilized

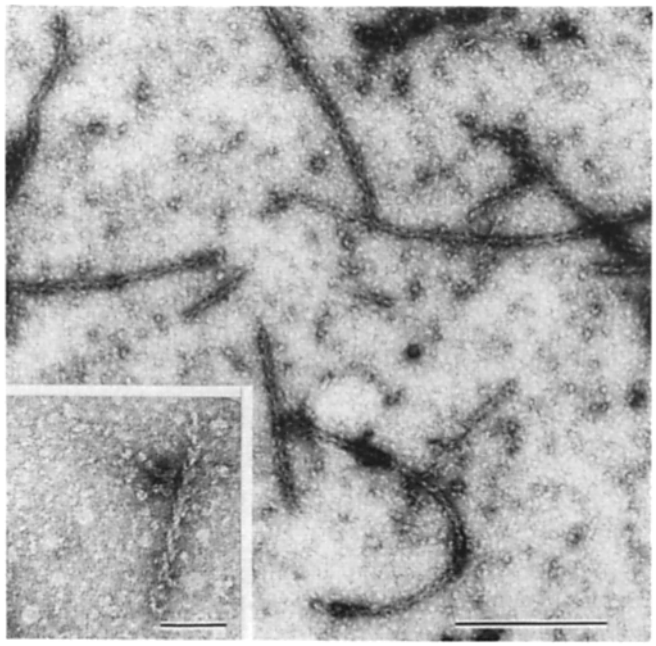

Figure 2. S-1 decorated and negatively stained axoplasmic MF. Axoplasm was extruded into buffer X containing 10 μM phalloidin and the axoplasm dispersed by depolymerizing the microtubules and neurofilaments with 0.6 M KI. The phalloidin-stabilized MF remained intact. These types of preparations were used to measure axoplasmic MF lengths. *Inset*, an example of an S-1–decorated MF at higher magnification. Bars, 0.1 μm.

axoplasm was dispersed, spread on a grid, and negatively stained. The microtubules and neurofilaments were removed with 0.6 M KI, and the MF were decorated with S-1 (Fig. 2). Control preparations with purified rabbit skeletal muscle actin indicate that our preparative methods did not artificially produce short MF (data not shown). The length–frequency distribution of axoplasmic MF is shown in Fig. 3 *A* representing 760 filaments from three axons. The filaments had a number average length of 0.55 μm and a weight average length of 0.74 μm. (A 0.55-μm-long filament contains ~200 actin monomers).

Morris and Lasek (1984) have proposed that 60% of the axonal MF are inherently stably polymerized. To selectively examine these MF, axoplasm was extracted for several hours in buffer X without phalloidin. This procedure eliminates any MF in equilibrium with monomer and retains the stable MF (Morris and Lasek, 1984). Fig. 3 *B* is the length–frequency distribution for 120 stable filaments from two axons. These filaments had a number average length of 0.79 μm (~286 monomers) and a weight average length of 1.14 μm. The mean lengths of the stable MF (Fig. 3 *B*) are on the average longer than the total population (Fig. 3 *A*) and the Kolmogorov–Smirnov test predicts that the two length distributions are significantly different ($p < 0.001$; Siegel, 1956).

Microfilament Distribution in Intact Axoplasm by Light Microscopy

To analyze the overall distribution of the MF in axoplasm, whole mounts of axoplasm were stained with rhodamine-phalloidin, which selectively stains MF (Wulf et al., 1979). Rhodamine-phalloidin–stained axoplasm contained fluores-

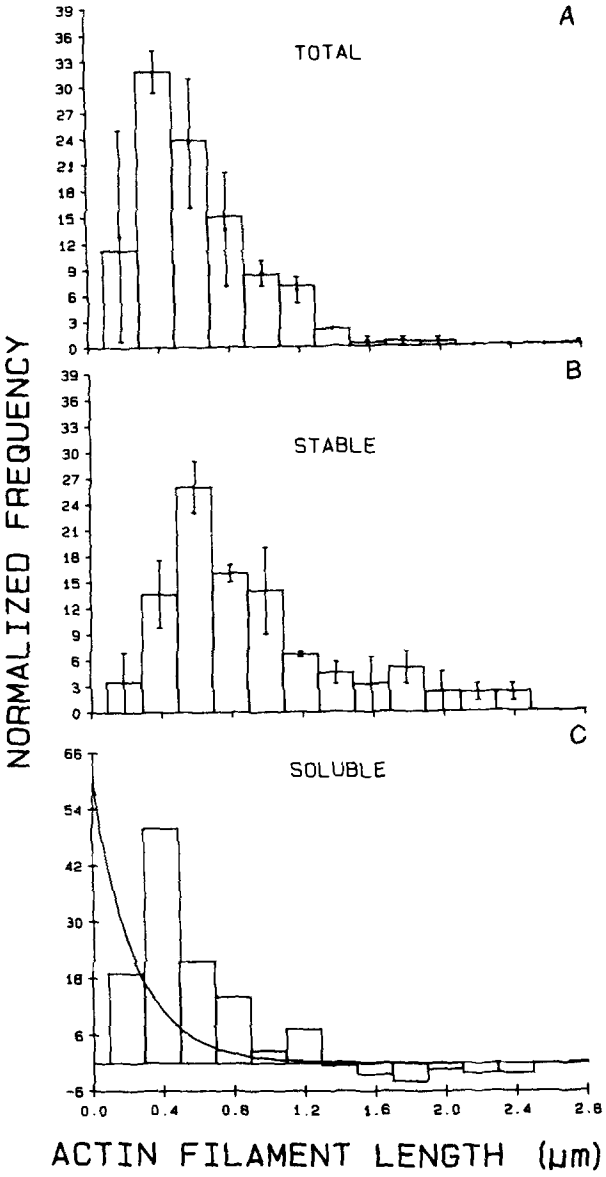

Figure 3. Distributions of axoplasmic MF lengths. (*A*) The distribution of lengths for the total axoplasmic MF was obtained from axoplasm that had been treated with 10 μM phalloidin to stabilize both the soluble and stable MF. The lengths for 640 MF (± range) from 3 different axoplasms are shown. (*B*) The distribution of lengths for only the stable MF was obtained from axoplasm that had been extracted without phalloidin for 4 h to selectively remove the soluble MF. The lengths for 120 stable MF (±range) prepared from two different axoplasms are shown. (*C*) The distribution of lengths for only the soluble MF was obtained by mathematically removing the population of stable MF (*B*) from the population of total MF (*A*). The distribution of the soluble MF lengths differs from the exponential distribution (represented as a continuous curve) that is expected for soluble MF polymerized in vitro.

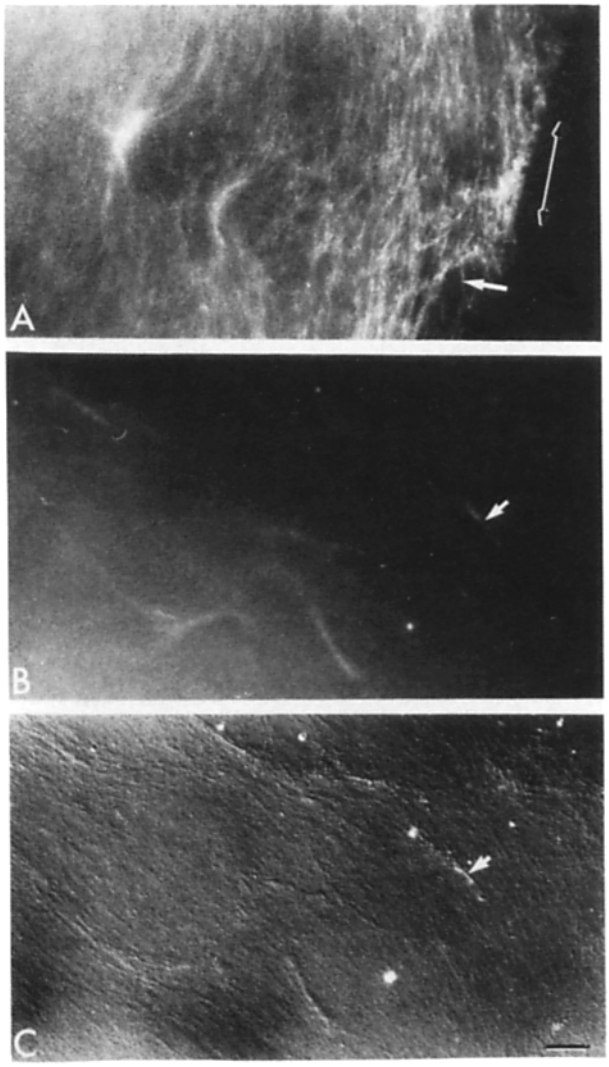

Figure 4. Axoplasm whole-mounts stained with rhodamine-phalloidin. (*A*) A fluorescent light micrograph of fixed axoplasm stained with rhodamine-phalloidin. The edge of the axoplasm is shown and the long axis of axoplasm indicated by the double arrow. Fluorescent stripes which are oriented along the axis of the axoplasm course through the axoplasm. The arrow marks an isolated stripe probably corresponding to a single bundle of MF that separated from the rest at the edge of the axoplasm. (*B*) Control axoplasm treated as in *A* but the buffer contained a 50-fold molar excess of unlabeled phalloidin in addition to rhodamine-phalloidin. (*C*) Diffraction-interference contrast micrograph of the same field as *B*. The arrow indicates a fold in the axoplasm corresponding to the fluorescent patch in *B*. Bar, 10 μm.

cent stripes or columns that ran along the long axis of the axon and were distributed fairly uniformly within the axoplasm (Fig. 4 *A*). Each column was ~1 μm wide and extended for many micrometers through the axoplasm. Individual columns were usually most clearly visible near the periphery of the axoplasm. Here, the axoplasm was very thin, and accordingly, the amount of image overlap between superimposed columns was minimized (Fig. 4 *A*).

To ensure that the fluorescent probe was binding to axonal MF, a 50-fold molar excess of unlabeled phalloidin was added to compete with the rhodamine-phalloidin for binding sites on the MF. The addition of the competing phalloidin eliminated the fluorescent stripes from the axoplasm (Fig. 4 *B*). Small fluorescent patches in these preparations corresponded to folds in the axoplasm (*arrow* in Fig. 4, *B* and *C*) that were also found in control axoplasm incubated in buffer alone (data not shown). These light microscopic results confirm those

obtained with the electron microscope and indicate that MF are concentrated in columnar domains that run parallel to the long axis of the axon.

The Spatial Organization of 4–6-nm MF in Axoplasm

Axoplasm that extruded directly into fixative contained an extensive interconnected network of small-diameter filaments (Fig. 5). At least two types of small-diameter filaments were found among the neurofilaments and microtubules. One type of filament had a diameter of 2–3 nm. These filaments were pervasive and apparently connected the microtubules and neurofilaments to adjacent structures (Fig. 5). The other type of filament was 4–6 nm in diameter (Fig. 5) and resembled the MF identified in negatively stained axoplasm. These 4–6 nm filaments were embedded in a dense granular and filamentous matrix that was associated with the microtubules.

This dense matrix tended to obscure the individual 4–6-nm filaments, even in thinnest sections. To reduce the interference from this matrix, we first stabilized the MF with 10 μM phalloidin and then extracted the soluble proteins. Extraction removed much of the dense matrix as well as many of the reticular 2–3-nm filaments revealing the 4–6 nm filaments (Fig. 5, *C* and *D*). These stereomicrographs also illustrate the bundles of microtubules that typically course longitudinally through the axoplasm. Most of the 4–6-nm filaments were located in the vicinity of microtubules and they were often aligned along the long axis of these microtubule bundles.

In Situ S-1 Decoration

Careful examination of axoplasm that had been treated with S-1 to decorate the MF in situ showed that the 4–6-nm filaments were no longer visible. This result suggested that the 4–6-nm filaments were coated with S-1. However, we did not observe the typical arrowhead pattern that characterizes S-1–decorated MF. Apparently, the numerous fine filamentous elements in axoplasm obscured the S-1 pattern. This problem was partially resolved by immersing axoplasm in a hypotonic buffer (buffer X diluted 1:1 with distilled water) so as to swell the structure of the axoplasm and separate the MF form adjacent filamentous cytoskeletal structure while conserving the overall architecture of the axoplasm (Allen et al., 1985; Vale et al., 1985). S-1 decorated filaments were easily identifiable in these preparations (Fig. 5 *B*). This observation and the observation that very few naked 4–6-nm MF were present in the S-1–decorated preparations further confirm the hypothesis that the 4–6-nm axoplasmic filaments contain actin.

Discussion

With only a few exceptions (LeBeux and Willemot, 1975; Alonso et al., 1981), studies of the morphological distribution of actin MF in axons have focused on the axonal cortex and these studies have engendered the impression that MF are minor components of the inner axonal cytoskeleton (Pachter et al., 1984). By contrast, our results indicate that >92% of the axonal actin in the squid giant axon is located in the central axoplasm. Moreover, the results support the proposal by Morris and Lasek (1984) that 60% of this actin is filamentous.

MF Density at the Cortex and Center of the Axon

Why have the numerous MF of the inner axonal cytoskeleton been overlooked? The small diameter of the MF together with the thick surrounding matrix of granular and filamentous structures contributes to the difficulty of visualizing the microfilaments in axoplasm. Furthermore, the axonal MF are short polymers (0.5 μm on average), and this adds to the difficulty of observing them with the electron microscope (Maupin and Pollard, 1986). By extracting the axoplasm with an excess of buffer, we were able to remove some of the interfering soluble matrix components, and the MF were more visible. We found the MF in the inner regions of the axon are sparsely distributed and are usually separated from each other. By contrast, cortical MF form a compact network subjacent to the axonal plasma membrane (Hirokowa, 1982; Metuzals and Tasaki, 1978; Tsukita et al., 1986). The difference in the concentration and organization of the MF in these two regions may explain why studies using fluorescence microscopy have focused entirely on the MF in the axonal cortex.

Immunofluorescent studies with actin antibodies show that the periphery of vertebrate myelinated axons in situ are much more fluorescent than the inner regions (Hirokawa, 1982). The weak fluorescence from the inner axoplasm has either been ignored or considered a technical artifact. The fluorescence produced by rhodamine-phalloidin is also more intense in the cortex of sectioned squid giant axons than it is from the inner regions of these axons (unpublished observations). Clearly, when immunofluorescent preparations show faintly stained regions adjacent to brightly stained regions, it is not a safe assumption that the antigen in question is missing from the faintly stained region.

MF–Microtubule Interactions in the Axonal Cytoskeleton

Our results with rhodamine-phalloidin show that the MF of the inner axonal cytoskeleton are organized in columns that are arranged longitudinally with respect to the axis of the axon (Fig. 4). In the giant axon, the axonal microtubules are organized in longitudinal bundles that have the same size and organization as these fluorescent columns (Fig. 5; Hodge and Adelman, 1983; Metuzals et al., 1983). Furthermore, our electron microscopic observations indicate that MF are most numerous in the regions of the axon with microtubules. Based on these observations, we propose that the MF in the central region of the axon cluster together with the microtubules.

The hypothesis that MF are associated with microtubules in the central axon is supported by kinetic studies of cytoskeletal polymer transport in mammalian axons (McQuarrie et al., 1986). These transport studies suggest that MF are more directly coupled to microtubules than to neurofilaments (McQuarrie et al., 1986). Furthermore, studies of the reorganization of the cytoskeleton in axons treated with β,β′-Iminodipropionitrile indicate that MF retain their association with microtubules when the microtubules cluster at the center of the axon and the neurofilaments form a ring at the periphery of the axon (Papasozomenos et al., 1986). This association is also supported by studies with purified proteins that indicate that microtubule-associated proteins can couple the MF to microtubules (Griffith and Pollard, 1978;

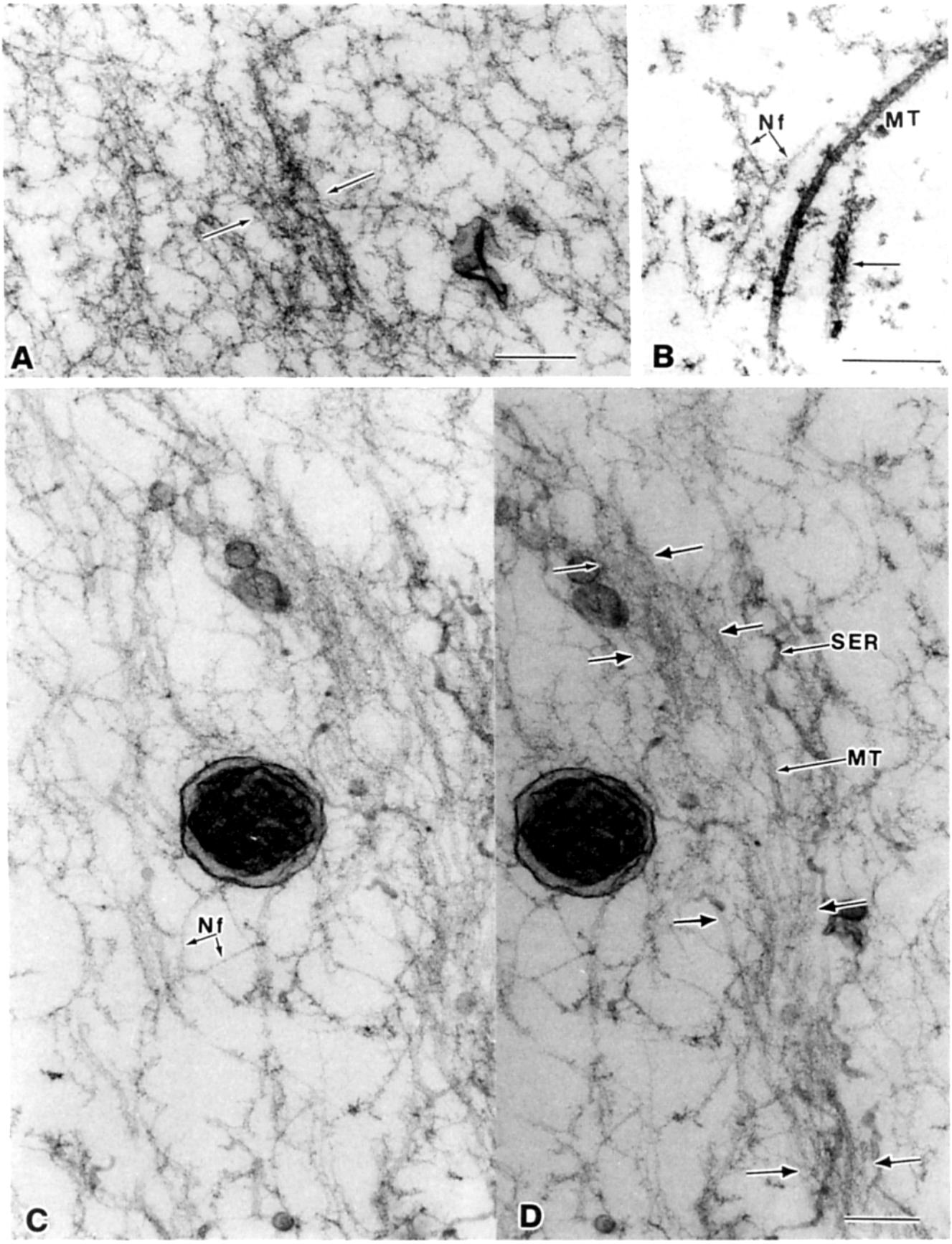

Figure 5. (*A*) Axoplasm extruded directly into fixative. Axoplasm contains dense regions associated with microtubules and these are arranged in bundles that course longitudinally with respect to the axis of the axon (*arrows*). These dense regions are surrounded by less

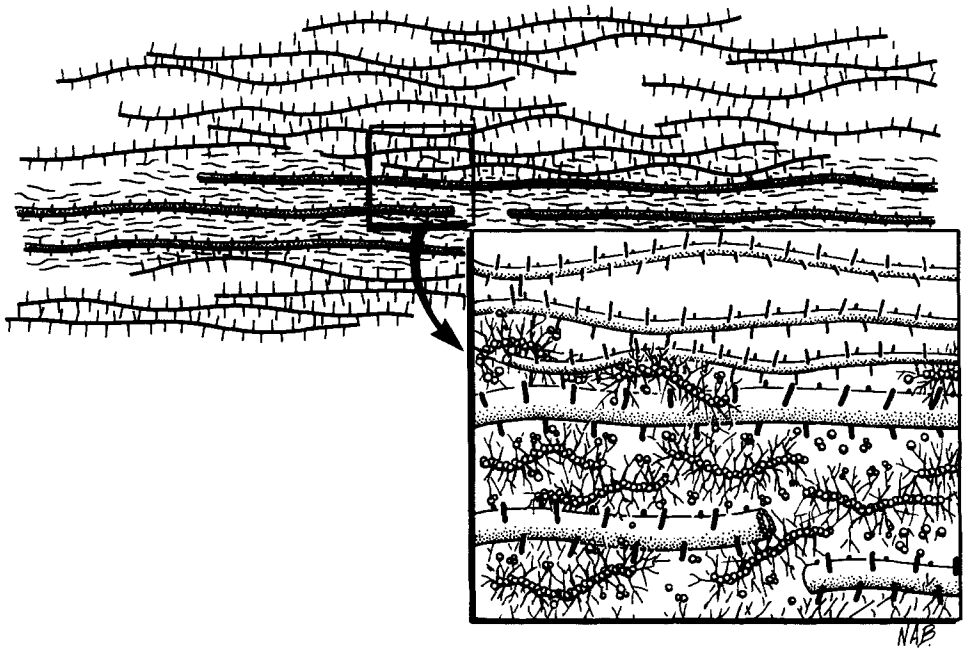

Figure 6. A model summarizing the basic organization of the axonal cytoskeleton in the central regions of the squid giant axon. The relative number and diameter of the actin MF, microtubules, and neurofilaments are depicted as they occur in the axoplasm. Note that the MF are much shorter than the microtubules but that they are much more abundant than the microtubules. In the magnified *inset* the dense reticular network surrounding the MF is included.

Sattilaro et al., 1981), and very short MF have also been demonstrated in the microtubule bundles of the mitotic spindle (Maupin and Pollard, 1986). Through such attachments to the microtubules, axonal MF may directly participate in the structural organization of the microtubule bundles in the axon.

The structural integrity of the MF that are associated with the microtubule bundles appears to be required for normal vesicle transport in the axon. For example, if axonal MF are depolymerized with DNase I or gelsolin, anterograde and retrograde vesicle transport is inhibited (Isenberg et al., 1980; Goldberg et al., 1980; Brady et al., 1984). Apparently, DNase I and gelsolin inhibit vesicle transport by disrupting the structural organization of the axoplasm, notably, the microtubule domains (Brady et al., 1984; Nemhauser and Goldberg, 1985). Based on these observations and our finding that MF are concentrated near microtubules, we propose that the MF have an important architectural role in the organization of axonal microtubule bundles.

Axonal MF Organize the Soluble Cytomatrix Proteins in Axons

In addition to their organizational role in the architecture of the microtubule bundles, MF also organize many proteins that are concentrated in the region of the microtubule bundles. Actin directly binds glycolytic enzymes and other soluble proteins (Clarke and Masters, 1975; Knull et al., 1980; Masters, 1984) and MF-associated proteins, such as spectrin, may provide secondary binding sites for the attachment of soluble proteins to the MF (Kakiuchi et al., 1982).

Because of their capacity to bind to many otherwise soluble proteins, MF may have an important role in the active transport of many of the soluble cytomatrix proteins in axons. For example, kinetic analyses of slow axonal transport demonstrate that soluble proteins, such as enolase and calmodulin move coordinately with the MF in slow component b (Brady et al., 1980). Based on these observations and others, Lasek et al. (1984) have proposed that MF are integral components of a "carrier complex" that transports soluble proteins within the axon. In support of this hypothesis, we found that axonal MF are normally surrounded by an electron-dense matrix of granular and filamentous proteins and that extraction of the soluble proteins with a physiological buffer removes these proteins from the regions surrounding the MF.

Metastable and Stable MF: Two Populations of Axonal MF

Morris and Lasek (1984) have proposed that axoplasmic actin exists in three forms: monomer, metastable MF, and stable MF. Our results confirm this proposal and demonstrate that the average lengths of the total population of MF (metastable + stable) are shorter than those of the stable population of MF (Fig. 3). Using the observation of Morris and Lasek (1984) that 50% of the MF are stable and the remainder

dense regions that contain primarily neurofilaments. In addition to the microtubules and neurofilaments, 4–6-nm MF are abundant in the microtubule regions and a reticular network of 2–3-nm filaments radiate from the polymers. (*B*) Axoplasm was swollen by extraction with half strength buffer X containing 10 μM phalloidin and then labeled with S-1. Swelling the axoplasm separates the cytoskeletal polymers and reveals the decorated actin MF (*arrow*), which is next to a microtubule (*MT*). A number of 10-nm neurofilaments are also shown. (*C* and *D*) Stereo electron micrograph of a relatively thick (0.2–0.25-μm-thick) section of axoplasm extracted 4 h in buffer X containing 10 μM phalloidin before fixation. Extraction removed most of the dense reticular matrix from the regions surrounding the microtubules. A mitochondrion lies next to a bundle of microtubules (*MT*) which is surrounded by a network of 4–6-nm MF (demarcated by *arrowheads*) that extends outside the area of stereo overlap. Viewed with stereo glasses, the 4–6-nm MF are more easily seen than in the unextracted axoplasm (compare with *A*). *Nf*, neurofilament; *SER*, smooth endoplasmic reticulum; *MT*, microtubules. Stereo tilt ± 7°. Bars: (*A*, *C*, and *D*) 0.2 μm; (*B*) 0.1 μm.

are metastable, we mathematically extracted the distribution of lengths for the metastable MF from the total population of MF (length of total × 2 − length of stable = length of metastable; Fig. 3 *C*). We calculate that 69% of the metastable MF have lengths of 0.4 μm or less. By contrast, only 20% of the stable MF are shorter than 0.4 μm. These results rule out the possibility that the stable MF are contained within longer MF with metastable ends. Instead, these observations indicate that the axonal cytoskeleton contains two distinct populations of MF: stable MF that are on average 0.79 μm long and metastable MF that are on average 0.41 μm long.

Regulation of MF Length in Axons

The shapes of the length distributions for both the metastable and stable populations of axonal MF differ from those obtained for purified actin polymerized in vitro. The length distribution of MF in vitro forms a continuous exponential curve (Fig. 3 *C*, based on data from Kawamura and Maruyuma, 1970). By contrast, the length distribution of the metastable MF in axoplasm peaks near 0.4 μm. Kawamura and Maruyama (1970) were able to generate peaks in the length distributions of MF by adding factors such as myosin aggregates that bind to the MF and affect their assembly. Our results are consistent with the hypothesis that the various proteins regulating MF length in vitro are also functioning in the cell. Based on this observation, we propose that the axonal MF are not simply at equilibrium with monomer in the axon but that another factor(s) influences MF length. Presumably, these factors are concentrated in the dense regions of the axoplasm where MF are clustered.

Conclusions

Fig. 6 schematically summarizes our proposal of the organization of the inner axonal cytoskeleton. Here, the MF are aligned in longitudinal columns, where they appear to be associated with microtubules. As with the short MF that are associated with microtubules in the mitotic spindle (Maupin and Pollard, 1986), the small size of the axonal MF has obscured these polymers in the electron microscope. Although the individual MF are relative short, the combined length of all of the MF in the axonal microtubule bundles is greater than the combined length of the microtubules. Through their many interactions with other proteins, such as metabolic enzymes and structural linkers, these numerous short MF have an essential role in the architecture and dynamic metabolism of the inner axonal cytoskeleton.

Received for publication 22 March 1988, and in revised form 26 April 1988.

References

Allen, R., D. Weiss, J. Hayden, D. Brown, H. Fujiwake, and M. Simpson. 1985. Gliding movement of and bidirectional transport along single native microtubules from squid axoplasm: evidence for an active role of microtubules in cytoplasmic transport. *J. Cell Biol.* 100:1736–1752.

Alonso, G., J. Gabrion, E. Travers, and I. Assenmacher. 1981. Ultrastructural organization of actin filaments in neurosecretory axons of the rat. *Cell Tissue Res.* 214:323–341.

Amos, L., R. Linck, and A. Klug. 1976. Molecular structure of flagellar microtubules. *In* Cell Motility. R. Goldman, T. Pollard, and J. Rosenbaum, editors. Cold Spring Harbor Laboratory, Cold Spring Harbor, New York. 847–868.

Atkinson, M., J. Morrow, and V. Marchesi. 1982. The polymeric state of actin in the human erythrocyte cytoskeleton. *J. Cell Biochem.* 18:143–155.

Brady, S., and R. Lasek. 1980. The axonal transport of nerve specific enolase and creatine phosphokinase: the axoplasmic matrix. *Cell.* 23:523–531.

Brady, S., R. Lasek, R. Allen, H. Lin, and T. Stossel. 1984. Gelsolin inhibition of fast axonal transport indicates a requirement for actin microfilaments. *Nature (Lond.).* 310:56–58.

Bray, D., and M. Bunge. 1981. Serial analysis of microtubules in cultured rat sensory axons. *J. Neurocytol.* 10:589–605.

Clarke, F., and C. Masters. 1975. On the association of glycolytic enzymes with structural proteins of skeletal muscle. *Biochim. Biophys. Acta.* 381: 37–46.

Cooper, J., and T. Pollard. 1982. Methods to measure actin polymerization. *Methods Enzymol.* 85:182–210.

Dancker, P., I. Low, W. Hasselbach, and T. Wieland. 1975. Interaction of actin with phalloidin: polymerization and stabilization of f-actin. *Biochim. Biophys. Acta.* 400:407–414.

Goldberg, D., D. Harris, B. Lubit, and J. Schwartz. 1980. Analysis of the mechanism of fast axonal transport by intracellular injection of potentially inhibitory macromolecules: Evidence for a possible role of actin filaments. *Proc. Natl. Acad. Sci. USA.* 77:7448–7452.

Griffith, L., and T. Pollard. 1978. Evidence for actin filament-microtubule interaction mediated by microtubule-associated proteins. *J. Cell Biol.* 78: 958–965.

Heriot, K., P. Gambetti, and R. Lasek. 1985. Proteins transported in slow components a and b of axonal transport are distributed differently in the transverse plane of the axon. *J. Cell Biol.* 100:1167–1172.

Hirokawa, N. 1982. Cross-linker system between neurofilaments, microtubules, and membranous organelles in frog axons revealed by the quick-freeze, deep-etching method. *J. Cell Biol.* 94:129–142.

Hodge, A., and W. Adelman. 1983. The neuroplasmic lattice structural characteristics in vertebrate and invertabrate axons. *In* Structure and Function in Excitable Cells. Chang, Tasaki, Adelman, and Leuchtag, editors. Plenum Publishing Corp., New York. 75–111.

Isenberg, G., P. Shubert, and G. Kreutzberg. 1980. Experimental approach to test the role of actin in axonal transport. *Brain Res.* 194:588–593.

Kakiuchi, S., K. Sobue, K. Kanda, K. Morimoto, S. Tsukita, S. Tsukita, H. Ishikawa, and M. Kurokawa. 1982. Correlative biochemical and morphological studies of brain calspectin: a spectrin-like calmodulin-binding protein. *Biomed. Res.* 3:400–410.

Kawamura, M., and K. Maruyama. 1970. Electron microscopic particle length of f-actin polymerized *in vitro*. *J. Biochem.* 67:437–457.

Knull, H., W. Brostein, P. Desjardin, and W. Niehaus. 1980. Interaction of selected brain glycolytic enzymes with a f-actin-tropomyosin complex. *J. Neurochem.* 34:222–225.

Korn, E. 1982. Actin polymerization and its regulation by proteins from nonmuscle cells. *Physiol. Rev.* 62:672–737.

Lasek, R., J. Garner, and S. Brady. 1984. Axonal transport of the cytoplasmic matrix. *J. Cell Biol.* (Suppl.):212–221.

LeBeux, Y., and J. Willemot. 1975. An ultrastructural study of the microfilaments in rat brain by means of heavy meromysin labeling. I. The perikaryon, the dendrites and the axon. *Cell Tissue Res.* 160:1–36.

Letourneau, P. 1983. Differences in the organization of actin in the growth cones compared with the neurites of cultured neurons from chick embryos. *J. Cell Biol.* 97:963–973.

Masters, C. 1984. Interactions between glycolytic enzymes and components of the cytomatrix. *J. Cell Biol.* (Suppl.):222–225.

Maupin, P., and T. D. Pollard. 1986. Arrangement of actin filaments and myosin-like filaments in the contractile ring and of actin-like filaments in the mitotic spindle of dividing HeLa cells. *J. Ultrastruct. Mol. Struct. Res.* 94:92–103.

McDonald, K. 1984. Osmium ferricyanide fixation improves microfilament preservation and membrane visualization in a variety of animal cell types. *J. Ultrastruct. Res.* 86:107–118.

McQuarrie, I., S. Brady, and R. Lasek. 1986. Diversity in the axonal transport of structural proteins: major differences between optic and spinal axons in the rat. *J. Neurosci.* 6:1593–1605.

Metuzals, J., and I. Tasaki. 1978. Subaxolemmal filamentous network in the giant nerve fiber of the squid (*Loligo pealei*) and its possible role in excitability. *J. Cell Biol.* 78:597–621.

Metuzals, J., A. Hodge, R. Lasek, and I. Kaiserman-Abramof. 1983. Neurofilamentous network and filamentous matrix preserved and isolated by different techniques from squid giant axon. *Cell Tissue Res.* 228:415–432.

Morris, J., and R. Lasek. 1982. Stable polymers of the axonal cytoskeleton: the axoplasmic ghost. *J. Cell Biol.* 92:192–198.

Morris, J., and R. Lasek. 1984. Monomer-polymer equilibria in the axon: direct measurement of tubulin and actin as polymer monomer in axoplasm. *J. Cell Biol.* 98:2064–2076.

Nemhauser, I., and D. Goldberg. 1985. Structural effects in axoplasm of DNase I, and actin depolymerizer that blocks fast axonal transport. *Brain Res.* 334:47–58.

Pachter, J., R. Liem, and M. Shelanski. 1984. The neuronal cytoskeleton. *Adv. Cell Neurobiol.* 5:113–142.

Papasozomenos, S. C., and M. R. Payne. 1986. Actin immunoreactivity localizes with segregated microtubules and membranous organelles and in the subaxolemmal region in the β, β′-iminodipropinitral axon. *J. Neurosci.* 6(12):3483–3491.

Sattilaro, R., W. Dentler, and E. LeCluyse. 1981. Microtubule-associated proteins (MAPs) and the organization of actin filaments in vitro. *J. Cell Biol.*

90:467–473.

Scordilis, S., and R. Adelstein. 1978. A comparative study of the myosin light chain kinases from myoblast and muscle sources. *J. Biol. Chem.* 253: 9041–9048.

Shaw, G., M. Osborn, and K. Weber. 1981. Arrangement of neurofilaments, microtubules and microfilament-associated proteins in cultured dorsal root ganglia cells. *Eur. J. Cell Biol.* 24:20–27.

Shen, B., R. Josephs, and T. Steck. 1984. Ultrastructure of unit fragments of the skeleton of the human erythrocyte membrane. *J. Cell Biol.* 99:810–821.

Siegel, S. 1956. Nonparametric Statistics For The Behavioral Sciences. McGraw-Hill Book Co., New York.

Spooner, B., and C. Holladay. 1981. Distribution of tubulin and actin in neurites and growth cones of differentiating nerve cells. *Cell Motil.* 1:167–178.

Tsukita, S., S. Tsukita, T. Kobyayashi, and G. Matsumoto. 1986. Subaxolemmal cytoskeleton in squid giant axon. II. Morphological identification of microtubule- and microfilament-associated domains of axolemma. *J. Cell Biol.* 102:1710–1725.

Vale, R., B. Schnapp, T. Reese, and M. Sheetz. 1985. Movement of organelles along filaments dissociated from the axoplasm of the squid giant axon. *Cell.* 40:449–454.

Weeds, A., and R. Taylor. 1975. Separation of subfragment-1 isoenzymes from rabbit skeletal muscle myosin. *Nature (Lond.).* 257:54–56.

Wulf, E., A. Deboben, F. Bautz, H. Faulstich, and T. Wieland. 1979. Fluorescent phallotoxin, a tool for the visualization of cellular actin. *Proc. Natl. Acad. Sci. USA.* 9:4498–4502.